

Thermoeconomic investigation on advanced Kalina power generation system

G. Uma Maheswari^a, N. Shankar Ganesh^{b,*}, Tangellapalli Srinivas^c, B.V. Reddy^d

^a Department of Computer Applications, School of Information Technology and Engineering, Vellore Institute of Technology, Vellore - 632014, Tamil Nadu, India

^b Department of Mechanical Engineering, Kingston Engineering College, Vellore - 632059, Tamil Nadu, India

^c Department of Mechanical Engineering, Dr. B R Ambedkar National Institute of Technology, Jalandhar, Punjab -144001, India

^d Department of Mechanical and Manufacturing Engineering, Faculty of Engineering and Applied Science, Ontario Tech University (UOIT), Oshawa, ON, Canada, L1H 7K4

ARTICLE INFO

Article history:

Received 20 May 2020

Received in revised form 20 September 2020

Accepted 28 September 2020

Available online 6 October 2020

Keywords:

Thermoeconomic

Physical exergy

Chemical exergy

Kalina cycle

Product

Fuel

Exergoeconomic factor

ABSTRACT

This work presents energy, exergy, and thermoeconomic analysis of an advanced Kalina power generation system. In every key component of the proposed system, cost-balance and auxiliary equations are typically developed which is solved efficiently through MATLAB coding. The cost-effectiveness of the entire system is assessed by the determination of thermoeconomic variables for the individual components. The energy analysis of the advanced Kalina cycle system (AKCS) proves marginal improvement to the medium temperature heat recovery Kalina cycle system (KCS). The relative cost difference in HE₅, turbine, HE₆, and condenser are quite larger than other components of AKCS emphasizing more focus on these components is required. The low values of HE₅ (11.77 %) and pump1, P₁ (13.33 %) insist that the performance of these two components has to be improved by capital investment into a better and improved design. The energy performance maximizes at operating conditions of 45 bar turbine inlet pressure, 72–74 °C separator inlet temperature, 0.94 ammonia concentration at the condenser and 0.83 separator inlet concentration. The thermoeconomic performance minimizes at operating conditions of 30 bar turbine inlet pressure, 68 °C separator inlet temperature, 0.89 ammonia concentration at the condenser and 0.79 separator inlet concentration.

© 2020 Published by Elsevier Ltd. This is an open access article under the CC BY-NC-ND license (<http://creativecommons.org/licenses/by-nc-nd/4.0/>).

1. Introduction

The utilization of efficient energy is an essential need in the industry sectors. Demand in the energy need is not easily measurable as it depends on population growth. The increase in energy dependence is upon the increased rational of industries. The environment need is an important measure against the rapid growth of innovative technologies from the industries. Modi et al. (2016) have reported a power generation cycle suitable work at high temperatures using an ammonia-water mixture as a working fluid. Kalina cycle proves to be the best power generation cycle at low-temperature applications due to its non-isothermal boiling and cooling tendency. Kalina cycle using an ammonia-water mixture is proposed as the most favorable alternatives for generating power from low-temperature geothermal energy hot source and energy from renewable sources (Zare and Palideh, 2018). The proposed model utilizes the waste heat of a Kalina cycle in thermoelectric generators. The irreversibility between

thermal oil from the solar collector and ammonia-water mixture working fluid of the Kalina cycle is minimized due to the variable boiling and condensation nature of mixture (Wang et al., 2013). The proposed system claims 8.54% of thermal efficiency at turbine inlet conditions of 18 bar and 106 °C.

Cao et al. (2018) compared the Kalina-Flash cycle (KFC) with Kalina cycle (KC) in thermodynamic and economic aspects and concluded that KFC is superior to KC. The thermodynamic properties have been obtained from software REFPROP 9.1. Optimum solutions to both KC and KFC have been resulted in using Pareto frontier solutions. Using geothermal source, a Kalina cycle generating power has been investigated through energy equation solver (EES) software (Fallah et al., 2016). To know the improvement possibility of the proposed system components, an advanced exergy analysis has been proposed. Condenser seeks a higher preference for improvement as per the advanced exergy analysis concern. Junior et al. (2019) have conducted cost analysis on the Kalina cycle generating power from waste heat recovery from the cement industry. The authors have optimized the system performance using a genetic algorithm. The sink condition considered in the proposed work is 22 °C. The system claims 23.3%

* Corresponding author.

E-mail address: nshankar_g@rediffmail.com (N. Shankar Ganesh).

of first law efficiency at turbine operating conditions of 370 °C and 77 bar.

Kalina cycle system utilizing subcritical coal-fired waste heat to generate power (Khankari et al., 2016). The proposed cycle generates net cycle efficiency of 2.58% with electric power of 13.49 MW. The authors have reported that a higher mass fraction of ammonia will result in improved performance. Avoiding accidents at the Kalina power system is to set an appropriate control strategy and inspecting the respective off-design performance (Wang, Wang, Dai, and Zhao) (Wang et al., 2017). The off-design performance has been improved by providing a modified sliding pressure controller. The power and energy efficiency performance reduce with the increment in sink temperature. Mehrpooya et al. (2019) have integrated solar flat plate collector (FPC) system with a Kalina cycle and biogas. The exergy efficiency of the combined system is reported as 92.36% with the major exergy destruction results from FPC. The authors have suggested that nano-enhanced fluids to transfer to heat will increase the characteristics of heat transfer. Geothermal sources have been considered as a suitable option to generate power, heating and cooling (Dhahad et al., 2020). Energy analysis and conventional exergy analysis have been performed in a combined cooling and Kalina power generation system. Mahmoudi et al. (2016) has performed economic and thermodynamic analysis in an integrated Kalina cycle and gas turbine-modular helium reactor. Exergy destruction ratio, exergy destruction cost and exergoeconomic factor are the parameters proposed for exergoeconomic investigation.

Ghaebi et al. (2018a) performed an investigation into a cascade Kalina cycle utilizing geothermal energy and liquefied natural gas as heat source and sink. The authors have examined single and multi-objective optimizations with a genetic algorithm. With a large expansion ratio of turbines, the investment cost is high. The exergy destruction reports being huge at the heat exchanger (II). Parikhani et al. (2019) has proposed a power generation cycle with ammonia-water as a working fluid with improved performance on an efficiency basis, utilizing the waste heat rejected from the gas turbine modular helium reactor. Conventional exergy analysis has been carried out in the system and concluded that the major exergy destruction results in the reactor. Cao et al. (2014) has conducted a parametric analysis in a regenerative Kalina cycle powered by biomass. Details of potential work vanished due to irreversibility have not been provided by energy analysis. Conventional exergy analysis provides the losses contributing to a particular component resulting in poor performance. The information about thermodynamic and economic ones is provided by thermoeconomics which is an integration of exergy analysis and economic analysis (Ozahi and Tozlu, 2020). The authors have formulated the cost balance equation and auxiliary equation using specific exergy costing (SPECOC). The energy from a solid waste power plant at a temperature of 566 °C is utilized by a Kalina cycle for generating power. Yu et al. (2020) has utilized geothermal resources effectively to generate power in a proposed integrated Kalina and transcritical CO₂ cycle. The performance of the integrated system has been reported as higher than the individual performances. The major exergy destruction occurs to the condenser and evaporator of the system components. To determine the cost of irreversibilities and the cost of investment, advanced exergy analysis has been proposed to a solar-driven Kalina cycle (Mehrpooya and Mousavi, 2018). The absorber is reported to have a high exergy destruction cost rate. Kahraman et al. (2019) have presented thermodynamic and thermoeconomic analysis of the organic Rankine cycle. The author has solved the thermodynamic properties using Aspen HYSYS software. The proposed cycle claims a higher exergy destruction rate for the turbine II. Bahrapoury and Behbahania (2017) have optimized the proposed Kalina cycle with exergy

efficiency as the objective function. For optimizing the objective function, a genetic algorithm has been considered.

The technological restrictions of individual cycle components and system component details are disclosed by advanced exergy analysis. (Liu et al., 2019). In conventional exergy analysis, the real cycle components with irreversibility have been focused. The individual components exergy destruction, exergy efficiency and exergy destruction rate of the real cycle are reported by conventional exergy analysis. The conventional exergy analysis proposes the largest irreversibility loss in the cooling chamber due to the two-phase transition process of carbon dioxide. The determination of system components real cost savings and the cost impacts have been possessed beneficially by advanced exergoeconomic analysis in comparison with conventional analysis (Liu et al., 2020a). Exergoeconomic analysis assesses the unit exergy cost of individual components through well-defined cost generation processes. This is impossible with economic assessment or exergy analysis on an individual system. The monetary price associated with exergy destruction has been assigned by conventional exergoeconomic analysis. Larger exergy destruction reveals that the high investment cost of the *i*th component has to be reduced. The exergy efficiency has been increased by lowering the exergy destruction on components. The sum of the capital investment cost of the entire system has been assessed by economic analysis (Liu et al., 2020b). The genetic algorithm balances the disagreement between the thermodynamic performance and cost index, which has been considered to be a multi-objective process. To estimate the optimal value of two different objective functions multi-objective algorithm is utilized.

Abam et al. (2020) has investigated energy, exergy and economic (3E) analysis on the proposed Kalina power cooling cycle. Respective to resource management and sustainability, the 3E analysis provides a steady technical and economic judgment. Bagheri et al. (2019) have identified the real beginning of irreversibilities associated with the system. The authors have used Golden section method for resulting the finest value of the distribution ratio. Shirmohammadi et al. (2018) have identified the optimum performance of the system with genetic algorithm (GA). To perform high quality result, GA is used in the proposed system. The initial step in evaluating the exergoeconomic analysis of a thermal system is exergy analysis (Xu et al., 2020). Mohammadi et al. (2018a) has stated that exergy in evaluating the system's performance and better criterion. The losses developed due to internal irreversibility in a system is analyzed with exergy. The feasibility of a project proposed is measured by economic analysis. The computation of irreversibility in a system resulting to the losses is the exergy destruction (Safarian and Aramoun, 2015). Feng et al. (2019) have concluded that in assessing the optimal design parameters, exergoeconomic optimization performs major part.

From the review, it is revealed that the low-temperature power generation Kalina cycle has been received a lot more attention as it is well-suitable to generate power from renewable energy sources (solar, geothermal, etc.). Also, it can be seen that the thermoeconomic analysis provides useful information about the performance of the system in thermodynamic and economic aspects. As per our best knowledge, thermoeconomic analysis and conventional exergy analysis on the Kalina cycle system suitable for medium temperature applications have not been reported so far. The motivation of the present study is that the Kalina cycle using zeotropic mixture tends to boil and condense at a non-isothermal process favoring a reduction in irreversibility in a boiler and condenser. The parameters considered for investigation into performance measurement is increased from an additional degree of freedom by using a zeotropic mixture. In the earlier studies, Thermoeconomic analysis of the Kalina

cycle suitable for medium temperature applications for high sink temperature has not been presented. This study concentrates on the evaluation of these consequences. The main objective of this work is to thermoeconomically evaluate an advanced Kalina cycle (AKC) suitable to recover heat from medium temperature heat sources. The presented performance measures includes (1) Parametric investigation into the advanced Kalina cycle system, (2) Comparison of the present system performance with the existing system, (3) Thermoeconomic investigation into AKC. To the best of our knowledge, this is the first attempt on assessing a medium temperature Kalina cycle from thermoeconomic aspects. In this paper, Section 2 demonstrates the description of the AKC. Section 3 explains the first law, second law and thermoeconomic procedure for the proposed cycle. Section 4 presents the results from the parametric and thermoeconomic investigation on the AKC. Section 5 proposes the conclusion of this research work.

2. Description of the proposed system

Figs. 1a and 1b represents the configuration of medium temperature Kalina power generation systems. The advanced Kalina cycle power generation system is utilized with two solar heaters. Both systems have generated a higher mass flow rate of the turbine against simple Kalina cycle systems. The advanced Kalina power generation system has higher heat recovery in heat exchangers HE₁, HE₂, and HE₃ with the addition of a solar collector. In Fig. 1b, the saturated ammonia-water solution (state 7) is pressurized to the heat exchanger 1 (HE₁), the heat exchanger 2 (HE₂) and heat exchanger three (HE₃) by the pump (P2). The condensate from the condenser is admitted to the heat exchanger (HE₆) rather than passing through the parallel heat exchangers. This will gain the heat source of secondary solar heater (solar collector 2) thus providing high-temperature heat input to the HE₁ ensuring reduced primary requirement of the hot source. The process completes the power generation system. The system thus generates more supply of the stream to the turbine per unit mass flow rate of the stream considered at the condenser. The higher the supply of the turbine, the most expansion with increased net specific work resulting in higher overall performance. In the advanced Kalina cycle system, the first law and second law analysis have been performed to assess the suitable parameters resulting in better performance. In the Kalina power system, three variables have been considered for the parametric investigation into more flexibility in results as compared to a single component working fluid system. The Kalina system uses ammonia-water mixture as a working fluid which results in temperature, pressure, and concentrations as the three variables focusing on the improvement in the overall system performance.

The advanced Kalina cycle has been examined with a mixture of property values at a range of pressure and temperature values. Initially, the examination was carried with the regular system shown in Fig. 1a. The ammonia-water mixture properties are very important to examine the performance investigation. The temperature and pressure values of each state points have been evaluated using mass and energy balances. Finding the liquid and vapor concentration of the mixture concentration on the separator is resulted based on the bubble point and dew point correlations (Shankar Ganesh and Srinivas, 2017). Upon the evaluation of the thermodynamic properties, the parametric investigation is proposed to further recommendation. In this work, first law and second law analysis for the advanced Kalina power generation system is performed and compared with the regular Kalina cycle system. The advanced exergy analysis has been measured for the proposed system for further improvements in the performance.

3. First law analysis

3.1. Assumptions

In the present study, the following assumptions have been employed:

- (i) The advanced Kalina cycle system works at a steady-state condition with the ignorance of kinetic and potential energies (Gao and Chen, 2018).
- (ii) In the piping arrangement of the system, the heat losses and pressure drop have been neglected (Abdolalipouradi et al., 2019).
- (iii) The isentropic turbine and pump efficiencies are considered to be 90% (Braun et al., 2002).
- (iv) The mechanical efficiency of the turbine and pump has been considered to be 96% (Ganesh and Srinivas, 2013).
- (v) The atmospheric conditions of the proposed system are 1.013 bar pressure and 25 °C temperature (Mehrpooya et al., 2019).
- (vi) The throttling process is considered an isenthalpic process (Han et al., 2013).

The mass balance and energy balance equation for the advanced Kalina power generation system is provided below in Eq. (1).

The energy efficiency of the advanced Kalina cycle system (AKCS) is (Maheswari G. Uma and Shankar Ganesh, 2020),

$$\eta_{KC} = \frac{\dot{m}_1(h_1 - h_2) - [\dot{m}_{11}(h_{11} - h_{10}) + \dot{m}_{22}(h_{22} - h_7)]}{\dot{m}_1(h_1 - h_{31}) + \dot{m}_{21}(h_{21} - h_{20}) + \dot{m}_{20}(h_{20} - h_{19}) + \dot{m}_{14}(h_{16} - h_{15})} \times 100 \quad (1)$$

3.2. Mass and energy balance equations for AKCS

The mass and energy balance equations for AKCS is provided in Table 1.

Where C_p is the specific heat at constant pressure, kJ/kg K

3.3. Second law analysis

The maximum theoretical useful output of a system at equilibrium condition is exergy analysis (Ghaebi et al., 2018a). The specific exergy of the individual components of a thermal system is the addition of physical and chemical exergies.

The exergy rates of the physical and chemical at every state point in the AKCS are given in the following equations (Abdolalipouradi et al., 2019; Parikhani et al., 2020):

$$\dot{E}_{x_{ph,i}} = \dot{m}(h - h_0 - T_0(s - s_0))_i \quad (2)$$

$$\dot{E}_{x_{ch,i}} = \dot{m} \left(\left[\frac{ex_{ch,NH_3}^0}{M_{NH_3}} \right] x + \left[\frac{ex_{ch,H_2O}^0}{M_{H_2O}} \right] (1 - x) \right) \quad (3)$$

Where, the molecular weight of the individual components of ammonia and water are $M_{NH_3} = 17$, $M_{H_2O} = 18$, $\dot{E}_{x_{ph,i}}$ is the physical exergy, $\dot{E}_{x_{ch,i}}$ is the chemical exergy and 0 refers to the environmental condition (Parikhani et al., 2020).

Total exergy of the APKC components is provided in Eq. (4),

$$\dot{E}_{x_{total,i}} = \dot{E}_{x_{ph,i}} + \dot{E}_{x_{ch,i}} \quad (4)$$

Product exergy and fuel exergy in evaluating exergy destruction are the maximum theoretical work expected to produce in a system and required to produce ideal work (Ghaebi et al., 2018a).

$$\dot{E}_{x_{D,i}} = \dot{E}_{x_{F,i}} - \dot{E}_{x_{P,i}} \quad (5)$$

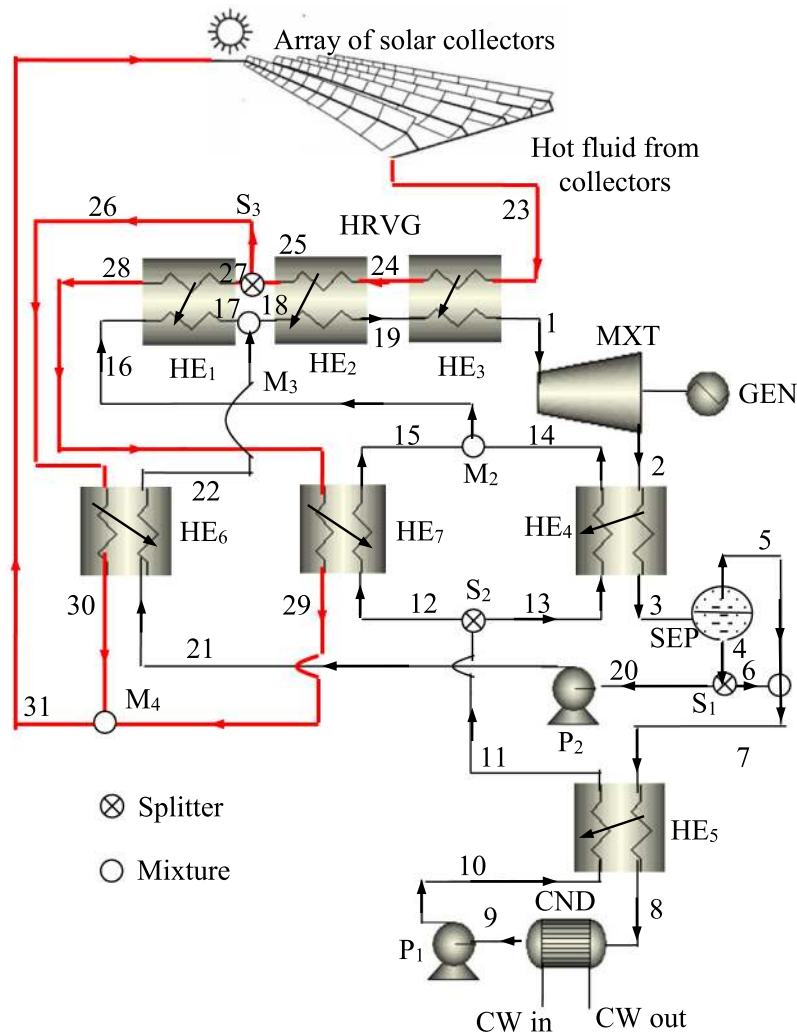


Fig. 1a. Schematic diagram of the medium temperature Kalina power generation system (KCS).

The exergetic efficiency of the individual component of AKPS is provided below (Mohammadi et al., 2018b),

$$\epsilon_i = \frac{\dot{E}_{Xp,i}}{\dot{E}_{Xf,i}} \times 100 \quad (6)$$

The exergy destruction ratio of the individual component of AKPS is provided in Eq. (7),

$$Y_{D,i} = \frac{E_{D,i}}{E_{D,Total}} \quad (7)$$

3.4. Fuel exergy of individual components

Table 2 provide the fuel exergy and product exergy of individual components.

3.5. Thermoeconomic analysis

Thermoeconomic analysis is an effective procedure in evaluating the combined exergy and economic principles (Parikhani et al., 2020). The cost balance equation and the auxiliary equation for the individual components are developed for determining the thermoeconomic analysis. The entire system is optimized with thermoeconomic analysis. To balance the cost of a system, total product cost rate ($\dot{C}_{p,tot}$) is determined as the addition of total fuel cost rate ($\dot{C}_{f,tot}$), total capital investment cost rate (\dot{Z}^{Cl}) and

the total operating and maintenance cost rate (\dot{Z}^{OM}) (Bejan et al., 1996). The exergetic efficiency and costs associated with exergy have been evaluated using a general methodology, specific exergy costing (SPECOC) approach (Lazzaretto and Tsatsaronis, 2006).

$$\dot{C}_{p,tot} = \dot{C}_{f,tot} + \dot{Z}_{tot}^{Cl} + \dot{Z}_{tot}^{OM} \quad (8)$$

The total cost rate of the *i*th component is the addition of the capital investment cost rate (\dot{Z}^{Cl}) and operating and maintenance cost rate (\dot{Z}^{OM}) (Ghaebi et al., 2018a; Bejan et al., 1996).

$$\dot{Z}_i = \dot{Z}_i^{Cl} + \dot{Z}_i^{OM} \quad (9)$$

The exergy costing relates the individual exergy stream (Bejan et al., 1996). The exergy transfer rate for the inlet stream, outlet stream, work transfer and heat transfer is expressed as in Eqs. (10)–(13),

$$\dot{C}_{inlet} = c_{inlet} \dot{E}_{inlet} \quad (10)$$

$$\dot{C}_{exit} = c_{exit} \dot{E}_{exit} \quad (11)$$

$$\dot{C}_{work} = c_{work} W \quad (12)$$

$$\dot{C}_{heat} = c_{heat} \dot{E}_{heat} \quad (13)$$

Let c_i , c_e , c_w and c_q be the average costs per unit of exergy in dollars per gigajoule (\$/GJ).

The addition of the total cost of the inlet exergy stream of the individual components with the capital and other costs will

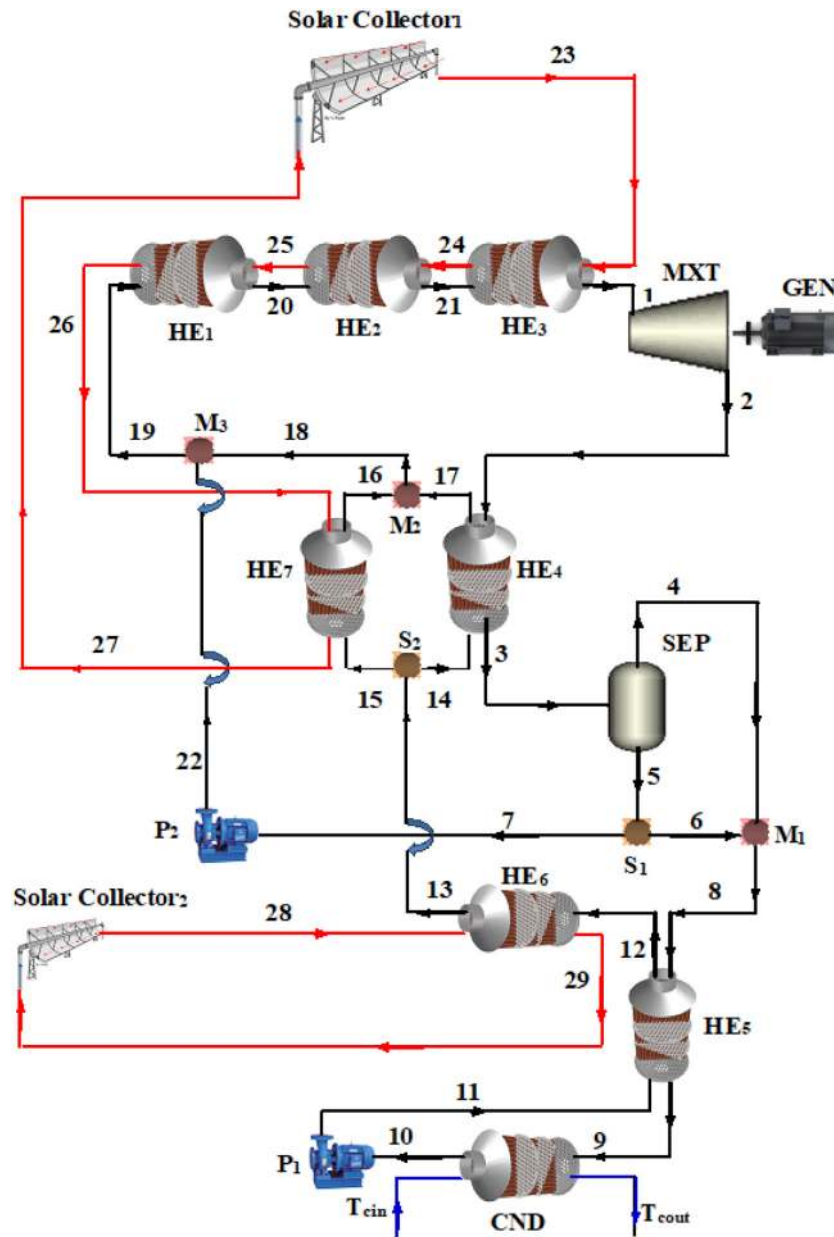


Fig. 1b. Schematic diagram of the advanced medium temperature Kalina power generation system (AKCS). P: condensate feed pumps; COND: condenser; T_{cin} : cooling water in; T_{cout} : cooling water out; HE: heat exchangers; M: mixers; MXT: mixture turbine; SEP: separator; and S: splitters.

be equal to the total cost of the output exergy stream of the individual components (Bejan et al., 1996).

$$\dot{C}_{heat,i} + \sum_{inlet} \dot{C}_{inlet,i} + \dot{Z}_i = \sum_{exit} \dot{C}_{exit,i} + \dot{C}_{work,i} \quad (14)$$

The cost of exergy destruction in every components of the system are determined as below (Ghaebi et al., 2018a):

$$\dot{C}_{D,i} = c_{p,i} \dot{E}X_{D,i} \text{ (if } \dot{E}X_{F,i} \text{ = constant)} \quad (15)$$

$$\dot{C}_{D,i} = c_{f,i} \dot{E}X_{D,i} \text{ (if } \dot{E}X_{P,i} \text{ = constant)} \quad (16)$$

The unit cost (specific cost) of fuel, $c_{f,i}$ and product, $c_{p,i}$ of the i th component in a system is, expressed in equations (44–45),

$$c_{p,i} = \frac{\dot{C}_{p,i}}{\dot{E}X_{P,i}} \quad (17)$$

$$c_{f,i} = \frac{\dot{C}_{f,i}}{\dot{E}X_{F,i}} \quad (18)$$

$\dot{C}_{p,i}$ and $\dot{C}_{f,i}$ are the exergy costs of product and fuel. The capital investment can be converted into cost rate as in the following equation:

$$\dot{Z}_i = CRF \times \frac{\phi_r \times 365 \times 24}{N} \times z_i \quad (19)$$

\dot{Z}_i is the cost rate of each component, z_i is the purchased equipment cost of the i th component, N is the annual unit operation hours =7000 (h), $\phi_r = 1.06$ (Ghaebi et al., 2018a), CRF is capital recovery factor,

$$CRF = \frac{k(1+k)^n}{(1+k)^n - 1} \quad (20)$$

Interest rate, $k = 0.15$ (Parikhani et al., 2020), Total operating period of the system in years, $n=20$ yr. (Parikhani et al., 2020)

Table 1
Mass and Energy balance equations for AKCS.

Components	Mass balance	Energy balance
HE ₁	$\dot{m}_{19} = \dot{m}_{20}, \dot{m}_{25} = \dot{m}_{26}$	$\dot{m}_{20} [h_{20} - h_{19}], \dot{m}_{25} C_p [T_{25} - T_{26}]$
HE ₂	$\dot{m}_{20} = \dot{m}_{21}, \dot{m}_{24} = \dot{m}_{25}$	$\dot{m}_{21} [h_{21} - h_{20}], \dot{m}_{24} C_p [T_{24} - T_{25}]$
HE ₃	$\dot{m}_{21} = \dot{m}_1, \dot{m}_{23} = \dot{m}_{24}$	$\dot{m}_1 [h_1 - h_{21}], \dot{m}_{23} C_p [T_{23} - T_{24}]$
HE ₄	$\dot{m}_2 = \dot{m}_3, \dot{m}_{14} = \dot{m}_{17}$	$\dot{m}_2 [h_2 - h_3], \dot{m}_{17} [h_{17} - h_{14}]$
HE ₅	$\dot{m}_8 = \dot{m}_9, \dot{m}_{11} = \dot{m}_{12}$	$\dot{m}_8 [h_8 - h_9], \dot{m}_{12} [h_{12} - h_{11}]$
HE ₆	$\dot{m}_{12} = \dot{m}_{13}, \dot{m}_{28} = \dot{m}_{29}$	$\dot{m}_{13} [h_{13} - h_{12}], \dot{m}_{28} C_p [T_{28} - T_{29}]$
HE ₇	$\dot{m}_{15} = \dot{m}_{16}, \dot{m}_{26} = \dot{m}_{27}$	$\dot{m}_{16} [h_{16} - h_{15}], \dot{m}_{26} C_p [T_{26} - T_{27}]$
MXT	$\dot{m}_1 = \dot{m}_2$	$\dot{m}_1 [h_1 - h_2]$
CND	$\dot{m}_9 = \dot{m}_{10}$	$\dot{m}_9 [h_9 - h_{10}], \dot{m}_{Tc,out} C_p [T_{c,out} - T_{c,in}]$
P ₁	$\dot{m}_{10} = \dot{m}_{11}$	$\dot{m}_{11} [h_{11} - h_{10}]$
P ₂	$\dot{m}_7 = \dot{m}_{22}$	$\dot{m}_{22} [h_{22} - h_7]$
M1	$\dot{m}_6 = \dot{m}_4 + \dot{m}_8$	$\dot{m}_6 h_6 = \dot{m}_4 h_4 + \dot{m}_8 h_8$
M2	$\dot{m}_{18} = \dot{m}_{16} + \dot{m}_{17}$	$\dot{m}_{18} h_{18} = \dot{m}_{16} h_{16} + \dot{m}_{17} h_{17}$
M3	$\dot{m}_{19} = \dot{m}_{22} + \dot{m}_{18}$	$\dot{m}_{19} h_{19} = \dot{m}_{22} h_{22} + \dot{m}_{18} h_{18}$
S1	$\dot{m}_6 = \dot{m}_5 - \dot{m}_7$	$\dot{m}_6 h_6 = \dot{m}_5 h_5 - \dot{m}_7 h_7$
S2	$\dot{m}_{15} = \dot{m}_{13} - \dot{m}_{14}$	$\dot{m}_{15} h_{15} = \dot{m}_{13} h_{13} - \dot{m}_{14} h_{14}$
SEP	$\dot{m}_5 = (1-VF) \dot{m}_3, \dot{m}_4 = (VF) \dot{m}_3$	

Table 2
Fuel and product exergy of individual components.

Components	Fuel exergy	Product exergy
Heat Exchanger	$\dot{E}_{F,HE} = (\dot{E}_{X_{HE,inlet}} - \dot{E}_{X_{HE,outlet}})_{hotstream}$	$\dot{E}_{P,HE} = (\dot{E}_{X_{HE,outlet}} - \dot{E}_{X_{HE,inlet}})_{coldstream}$
Turbine	$\dot{E}_{F,Turbine} = (\dot{E}_{X_{Turbine,inlet}} - \dot{E}_{X_{Turbine,outlet}})$	$\dot{E}_{P,Turbine} = \text{Specific Turbine work}$
Condenser	$\dot{E}_{F,Condenser} = (\dot{E}_{X_{Condenser,inlet}} - \dot{E}_{X_{Condenser,outlet}})_{hotstream}$	$\dot{E}_{P,Condenser} = (\dot{E}_{X_{Condenser,outlet}} - \dot{E}_{X_{Condenser,inlet}})_{coldstream}$
Pump	$\dot{E}_{F,Pump} = \text{Specific pump work}$	$\dot{E}_{P,Pump} = (\dot{E}_{X_{pump,inlet}} + \dot{E}_{X_{pump,outlet}})$
Mixing chamber	$\dot{E}_{F,Mixingchamber} = \dot{E}_{X_{mixingchamber,inlet1}} + \dot{E}_{X_{mixingchamber,inlet2}}$	$\dot{E}_{P,Mixingchamber} = \dot{E}_{X_{mixingchamber,outlet}}$
Separator	$\dot{E}_{F,Separator} = \dot{E}_{X_{Separator,inlet}}$	$\dot{E}_{P,Separator} = \dot{E}_{X_{Separator,liquid}} + \dot{E}_{X_{Separator,vapour}}$

Table 3
Investment cost rate of the components.

Components	Investment cost rate (Z _i)
Heat Exchanger	$Z_i = Z_R \left(\frac{A}{A_R}\right)^{0.6}$
Turbine	$Z_{MXT} = 4405 \times W_{Tur}^{0.7}$
Pump	$Z_{Pump} = Z_{R,Pump} \left(\frac{W_{Pump}}{W_{R,Pump}}\right)^{m_p} \left(\frac{1-\eta_{is,pump}}{\eta_{is,pump}}\right)^{n_p}$

3.6. Investment cost rate of the AKCS

From Table 3, the reference cost (Z_R), reference area (A_R) and overall heat transfer coefficient (U) for heat exchanger are considered to be \$16,000, 100 m² and 0.9 kW/m²K (Ghaebi et al., 2018b, 2017).

The reference cost (Z_R), reference area (A_R) and overall heat transfer coefficient (U) for vapor generator are considered to be \$17,500, 100 m² and 1.6 kW/m²K.

The reference cost (Z_R), reference area (A_R) and overall heat transfer coefficient (U) for the condenser are considered to be \$ 8000, 100 m² and 1.1 kW/m²K.

The constants Z_{R,Pump}, W_{R,Pump}, m_p, and n_p are \$ 2100, 10 kW, 0.26 and 0.5.

The separator and mixing chamber's investment costs have been neglected due to the small component cost (Ghaebi et al., 2018b).

Relative cost difference (r_i) of the system ith component is as below:

$$r_i = \frac{C_{P,i} - C_{F,i}}{C_{F,i}} \tag{21}$$

The important variable for assessing and optimizing system component is relative cost difference (Bejan et al., 1996).

The relative significance of each component's performance are provided by exergoeconomic factor f_i ,

$$f_i = \frac{\dot{Z}_i}{\dot{Z}_i + \dot{C}_{D,i}} \quad (22)$$

3.7. Cost based balance and auxiliary equations of the AKCS

Table 4 summarizes the cost balance equation and the auxiliary equation of each component of AKCS. Due to the minimum value of component cost, the investment costs of the separator and mixing chamber have been ignored (Ghaebi et al., 2018b).

The area for the heat exchangers, vapor generator and the condenser is evaluated utilizing logarithmic mean temperature difference and overall heat transfer coefficient (Ghaebi et al., 2018b),

$$Q = U_i A_i \text{LMTD}_i \quad (23)$$

3.8. Validation

The advanced Kalina power system is compared with the literature results from Ref. (Junior et al., 2019; Rashidi and Yoo, 2018) with the appropriate input conditions. The results of this work have higher first and second law performances as summarized in Table 5.

Table 6 shows the validated results of the present method against the reference values. The investment cost of the proposed system is lower than the reference considered.

4. Results and discussion

With the aforesaid assumptions, the proposed power generation system is simulated with MATLAB and Python coding on energy and exergy basis (Maheswari G. Uma and Shankar Ganesh, 2020). Parametric investigation into KCS and AKCS has been performed to identify the optimized conditions for both cases. Advanced exergy analysis followed by thermoeconomic analysis is evaluated for the AKCS.

4.1. Influence of separator inlet temperature and ammonia concentration at condenser in performance evaluation of AKCS and KCS

Variations on energy efficiency and exergy efficiency of KCS and AKCS with a change in separator inlet temperature and ammonia concentration in the condenser are shown in Figs. 2 and 3. As the ammonia concentration on the condenser increases the thermal efficiency are observed to increase almost steadily to both the systems until the optimum condition has achieved. The maximum value of efficiency for both the cases have resulted in 0.92 and 0.93 ammonia concentration at the condenser for KCS and AKCS respectively. Both the systems report higher performance to the same separator inlet temperature. At the same operating conditions, the maximum cycle efficiency is reported as 15% for KCS and 15.73% for AKCS at 72 °C separator temperature. The vapor generation of the mixture increases from an increase in separator inlet temperature. This produces a higher amount of ammonia vapor to the turbine resulting in higher performance at high separator inlet temperature. Increasing the ammonia concentration of the condenser beyond the optimum condition will result in more vapor concentration on low liquid concentration less enough to condense at required operating conditions in the condenser. The exergy efficiency trends are similar to energy efficiency performance variations.

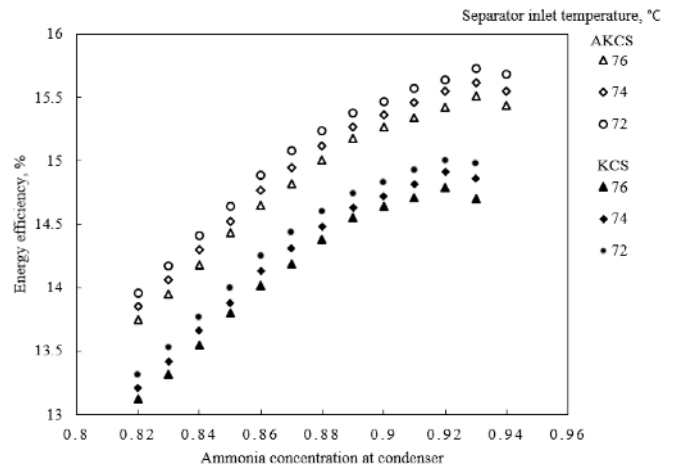


Fig. 2. Variation of energy performance with ammonia concentration at condenser and separator inlet temperature for KCS and AKCS.

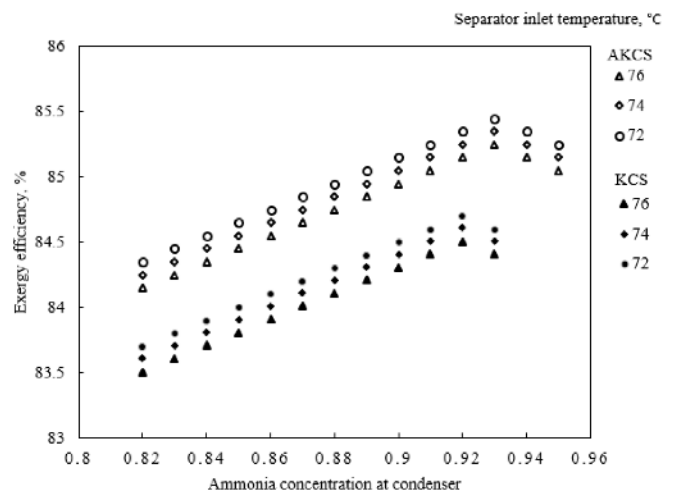


Fig. 3. Variation of exergy performance with ammonia concentration at condenser and separator inlet temperature for KCS and AKCS.

4.2. Influence of separator inlet temperature and separator inlet concentration on total product cost of AKCS

Fig. 4 shows the variations of AKCS product cost with separator inlet temperature and separator inlet concentration. For the studied working fluid, the product cost is minimized at an optimum value of the separator inlet temperature and concentration. The product cost optimize at lower separator inlet concentration. The lowest product cost records of 0.79 separator inlet concentration and 75 °C separator inlet temperature. The higher the $C_{p, total}$ value of high separator inlet concentration is due to the higher \dot{Z}_i value of heat exchanger as with reduced area. The total product cost reported to the literature in a high pressure on 71.2 bar and generator temperature of 450 K as 173 \$/GJ for the DEAR/Kalina cogeneration cycle (Shokati et al., 2018).

4.3. Influence of ammonia concentration at condenser and separator inlet temperature °C on total product cost of AKCS

The effect of ammonia concentration on the condenser and separator inlet temperature is examined on the total product cost of the AKCS and is shown in Fig. 5. Product cost is minimized at lower separator inlet temperature. It maximizes at 94% of the

Table 4
Cost balance and auxiliary equations of the individual components.

Components	Cost balance equation (CBE)	Auxiliary equations (AE)
HE1	$CBE_{HE1} = \dot{C}_{25} + \dot{C}_{19} + \dot{Z}_{HE1} = \dot{C}_{20} + \dot{C}_{26}$	$AE_{HE1} = C_{25} = C_{26}$
HE2	$CBE_{HE2} = \dot{C}_{24} + \dot{C}_{20} + \dot{Z}_{HE2} = \dot{C}_{21} + \dot{C}_{25}$	$AE_{HE2} = C_{25} = C_{26}$
HE3	$CBE_{HE3} = \dot{C}_{23} + \dot{C}_{21} + \dot{Z}_{HE3} = \dot{C}_1 + \dot{C}_{24}$	$AE_{HE3} = C_{23} = C_{24}$
HE4	$CBE_{HE4} = \dot{C}_2 + \dot{C}_{14} + \dot{Z}_{HE4} = \dot{C}_3 + \dot{C}_{17}$	$AE_{HE4} = C_2 = C_3$
HE5	$CBE_{HE5} = \dot{C}_8 + \dot{C}_{11} + \dot{Z}_{HE5} = \dot{C}_9 + \dot{C}_{12}$	$AE_{HE5} = C_8 = C_9$
HE6	$CBE_{HE6} = \dot{C}_{28} + \dot{C}_{12} + \dot{Z}_{HE6} = \dot{C}_{29} + \dot{C}_{13}$	$AE_{HE6} = C_{28} = C_{29}$
HE7	$\dot{C}_{26} + \dot{C}_{15} + \dot{Z}_{HE7} = \dot{C}_{16} + \dot{C}_{27}$	$AE_{HE7} = C_{26} = C_{27}$
MXT	$CBE_{MXT} = \dot{C}_1 + \dot{Z}_{Tur} = \dot{C}_2 + \dot{C}_{w,Tur}$	$AE_{MXT} = C_{w,Tur} = C_w$
CND	$CBE_{CND} = \dot{C}_9 + \dot{C}_{Tcin} + \dot{Z}_{CND} = \dot{C}_{10} + \dot{C}_{Tcout}$	$AE_{CND} = C_9 = C_{10}$
P ₁	$CBE_{P1} = \dot{C}_{10} + \dot{C}_{WP1} + \dot{Z}_{P1} = \dot{C}_{11}$	$AE_{P1} = C_{WP1} = C_w$
P ₂	$CBE_{P2} = \dot{C}_7 + \dot{C}_{WP2} + \dot{Z}_{P2} = \dot{C}_{22}$	$AE_{P2} = C_{WP2} = C_w$
M1	$CBE_{M1} = \dot{C}_4 + \dot{C}_6 + \dot{Z}_{M1} = \dot{C}_8$	–
M2	$CBE_{M2} = \dot{C}_{16} + \dot{C}_{17} + \dot{Z}_{M2} = \dot{C}_{18}$	–
M3	$CBE_{M3} = \dot{C}_{22} + \dot{C}_{18} + \dot{Z}_{M3} = \dot{C}_{19}$	–
SEP	$CBE_{SEP} = \dot{C}_3 + \dot{Z}_{SEP} = \dot{C}_4 + \dot{C}_5$	$AE_{SEP} = C_2 = C_3$

Table 5
Validation of the present results with the literature.

Parameter	Present work	Reference (Junior et al., 2019)	Reference (Rashidi and Yoo, 2018)
Turbine inlet temperature, °C	190	371.64	280
High pressure, bar	45	77.5	15
Separator inlet concentration	0.82	0.85	0.73
Flow rate of hot source, kg/s	1.238	4.204	1.3062
Cycle efficiency, %	15.56	23.33	13
Exergy efficiency, %	70	47.80	69.83
Net power, kW	253.89	2429	408.76
Pinch point temperature difference at HE ₃ , (°C)	8	18	10

Table 6
Comparison of the main parameters of the exergy analysis of this paper with the Mehrpooya and Mousavi (2018), Mahmoudi et al. (2016).

Parameter	Results of AKCS	Reference results (Mehrpooya and Mousavi, 2018)	Reference results (Mahmoudi et al., 2016)
Turbine inlet temperature, °C	190	371.64	280
High pressure, bar	45	77.5	15
$\dot{C}_{D,Overall}$, \$/hr	6	4.26	712.64
$C_{p,overall}$, \$/GJ	131.12	204.35	–
$\dot{E}_{D,Overall}$, kW	215	288	21927
$\dot{Z}_{D,Overall} + \dot{C}_{D,Overall}$, \$/hr	0.93	13.13	983.12

ammonia concentration on the ammonia water mixture. Due to the high heat exchanger area and input of heat exchanger and turbine, the investment cost rate increases resulting in high product cost at higher separator inlet temperature. The total product cost claims maximum of 144 \$/GJ at 0.93 ammonia concentration on the condenser and 78 °C separator inlet temperature. The total product cost rate of 0.662179 \$/MJ was reported on 15 bar turbine inlet pressure and 280 °C turbine inlet temperature for the Kalina cycle (Rashidi and Yoo, 2017). At the highest temperature in the cycle of 192.3 °C and 50 bar pressure, the literature results reported as 10.1 \$/GJ of overall product cost rate for a compressor pressure ratio of 2 in a combined gas turbine-modular helium reactor – augmented Kalina cycle (Mahmoudi et al., 2016).

4.4. Influence of ammonia concentration at condenser and turbine inlet pressure, bar in total product cost of AKCS

The effects on the total product cost of AKCS are shown in Fig. 6 with the effect of turbine pressure and ammonia concentration at the condenser. The product cost of the system minimizes at lower ammonia concentration on the condenser and turbine inlet pressure. With the increase in turbine pressure, the turbine unit cost increases in the effect of Rankine principle, hence larger total cost. The increase in total product cost is mainly with the large size of the equipment of AKCS.

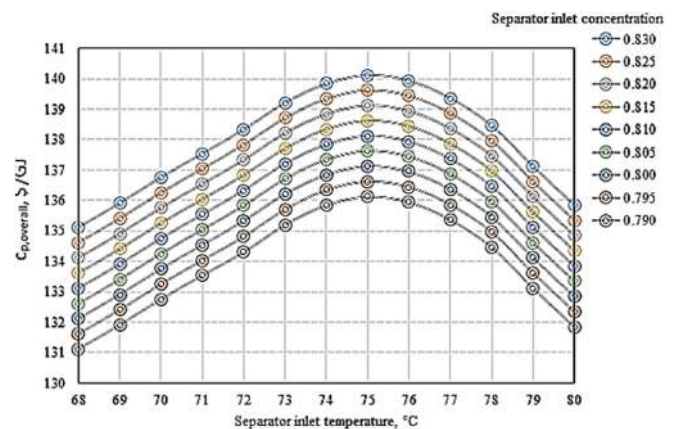


Fig. 4. Variation of the total product cost with separator inlet temperature and separator inlet concentration of AKCS.

4.5. Influence of ammonia concentration at condenser, turbine inlet pressure, bar, separator inlet concentration, separator inlet temperature, °C, on the overall cost of exergy destruction of AKCS

The overall cost of exergy destruction with a change in ammonia concentration on the condenser, turbine inlet pressure,

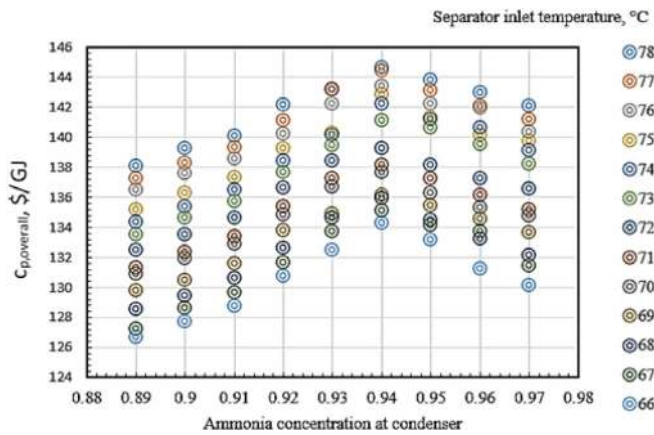


Fig. 5. Variation of total product cost with ammonia concentration at condenser and separator inlet temperature, °C of AKCS.

separator inlet concentration, and separator inlet temperature have been presented in Fig. 7a, 7b & 7c. The amount of $\dot{C}_{D,Overall}$, increases from an increase in separator inlet temperature. The components with a larger value of \dot{C}_D should be monitored exergoeconomically as concerned with exergoeconomic analysis. In the present work components turbine, HE₄ and HE₅ have the largest value of \dot{C}_D . At an increase in turbine inlet pressure, the value of \dot{C}_D decreases from the turbine, HE₄ and HE₅ and increases in the remaining components. As the cost associated with the turbine is very high, the value of \dot{C}_D decreases as a result. The total cost rate is proportional to the product cost rate and exergy destruction rate. With an increase in separator concentration, the turbine inlet pressure remains unchanged which put into a reduction in the overall cost of exergy value of the individual components hence favoring a decrement in total cost rate. The total exergy destruction cost rate reported on 15 bar turbine pressure and 280 °C as $4.98E-05$ \$/s at Kalina power and cooling cycle with the ejector and $6.32E-05$ at Kalina power and cooling cycle (Rashidi and Yoo, 2018).

4.6. Influence of ammonia concentration at condenser, turbine inlet pressure, bar, separator inlet concentration, separator inlet temperature, °C, on total exergy destruction of AKCS

The overall exergy cost destruction rate of performance parameters variation is reported in Fig. 8. At lower parametric values the exergy destruction rate has been minimized. At lower

separator pressure for constant turbine concentration, the individual exergetic destruction cost of high-temperature heat recovery components and turbine will increase resulting in an increment in the amount of \dot{E}_D . Thus, an increase in the overall exergy destruction rate will have an increasing trend at increased parameters until the optimum value has been obtained. The minimum exergy destruction rate is attained at 168.36 kW, 138.22 kW and 128.16 kW at 0.74 separator inlet concentration, 0.85 ammonia concentration at the condenser, 30 bar turbine inlet pressure, and 80 °C separator inlet temperature. The overall exergy destruction rate reported on the literature is 80.29 kW at a minimum product cost value of high pressure on 113.6 bar and generator temperature of 460 K (Shokati et al., 2018) for DEAR/Kalina cogeneration cycle.

4.7. Influence of ammonia concentration at condenser, turbine inlet pressure, bar, separator inlet concentration, separator inlet temperature, °C, on the exergoeconomic parameter $(\dot{C}_D + \dot{Z}_D)_{overall}$ of AKCS

The behavior of the $\dot{C}_D + \dot{Z}_D$ is identical to the total exergy destruction rate of the AKCS as shown in Fig. 9. An increase in separator inlet temperature with constant separator inlet concentration, more than half of the $\dot{C}_D, overall$ of the AKCS results in HE and separator, hence the value of exergy destruction rate and its cost produces an increasing trend. The most $\dot{Z}_D, overall$ relies on the turbine and HE4. With the increment in \dot{Z} value for both the turbine and HE4, for AKCS, there will be an increment in $\dot{Z}_D, overall$. With these reasons, the value of $\dot{C}_D, overall + \dot{Z}_D, overall$ will increase. The minimum value of $\dot{C}_D + \dot{Z}_D$ parameter are attained at 0.93 \$/hr, 2.04 \$/hr, and 4.06 \$/hr at 0.82 separator inlet concentration, 0.85 ammonia concentration at the condenser, 30 bar turbine inlet pressure, and 68 °C separator inlet temperature. The minimum of $\dot{C}_D + \dot{Z}_D$ parameter reported on the literature for the Goswami cycle is 9.879 \$/hr, DEAR/Kalina cycle is 8.118 \$/hr, SAR/Kalina cogeneration cycle is 5.429 \$/hr and in AKCS is 4.06 /hr (Shokati et al., 2018).

Fig. 10 compares the individual components exergetic loss of AKCS and KCS. The exergy loss in individual components is the ratio of irreversibility in individual components to the exergy of hot fluid (Maheswari G. Uma and Shankar Ganesh, 2020). Both AKCS and KCS have resulted in more exergetic loss in the turbine, heat exchanger HE₄ and condenser. The turbine has higher exergy loss due to the result of the dissipation of heat in the expansion. Due to large irreversibility between hot and cold fluids, exergy loss more is HE₄. The exergy destruction is high for these components along with fuel cost rate. The exergetic loss in the components of a cycle recommends the scope for improvement

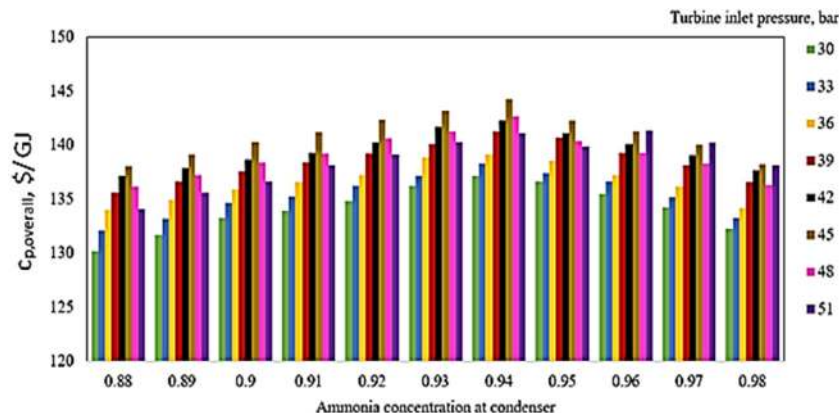


Fig. 6. Variation of total product cost with ammonia concentration at condenser and turbine inlet pressure, bar of AKCS.

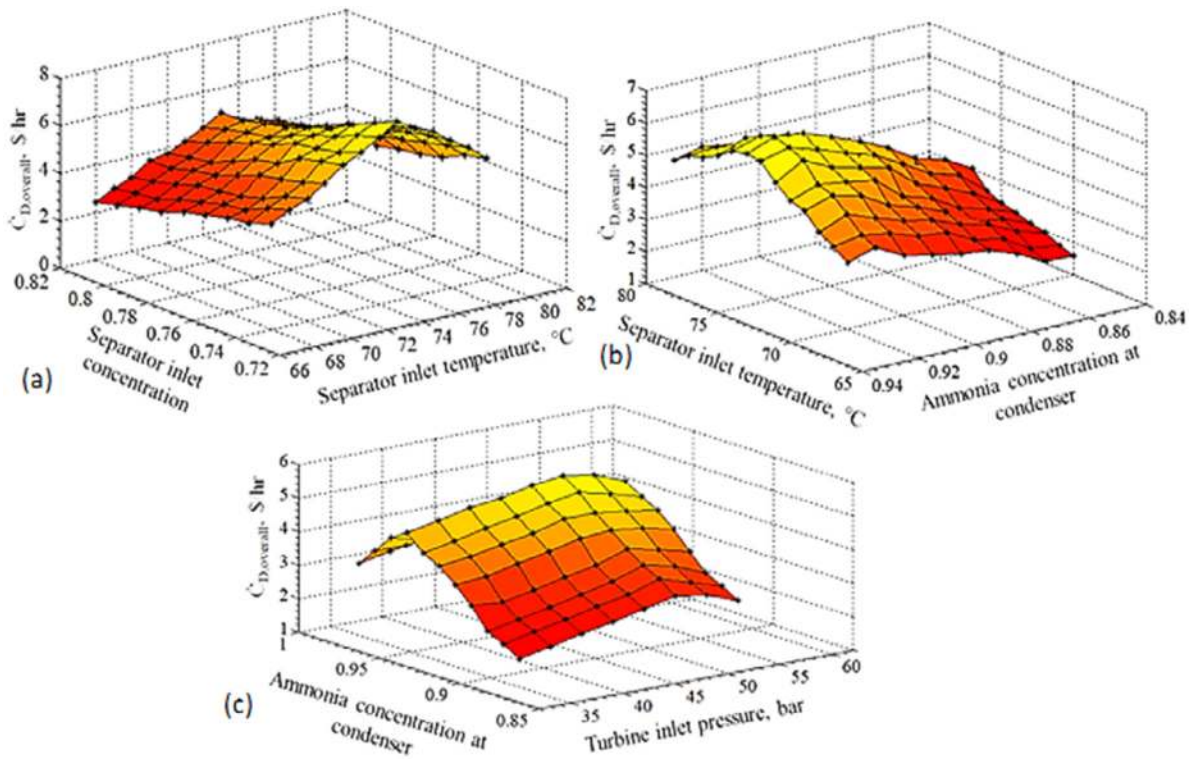


Fig. 7. Effects of (a) separator inlet concentration and separator inlet temperature, (b) separator inlet temperature and ammonia concentration at condenser and (c) ammonia concentration at condenser and turbine inlet pressure on overall cost of exergy destruction.

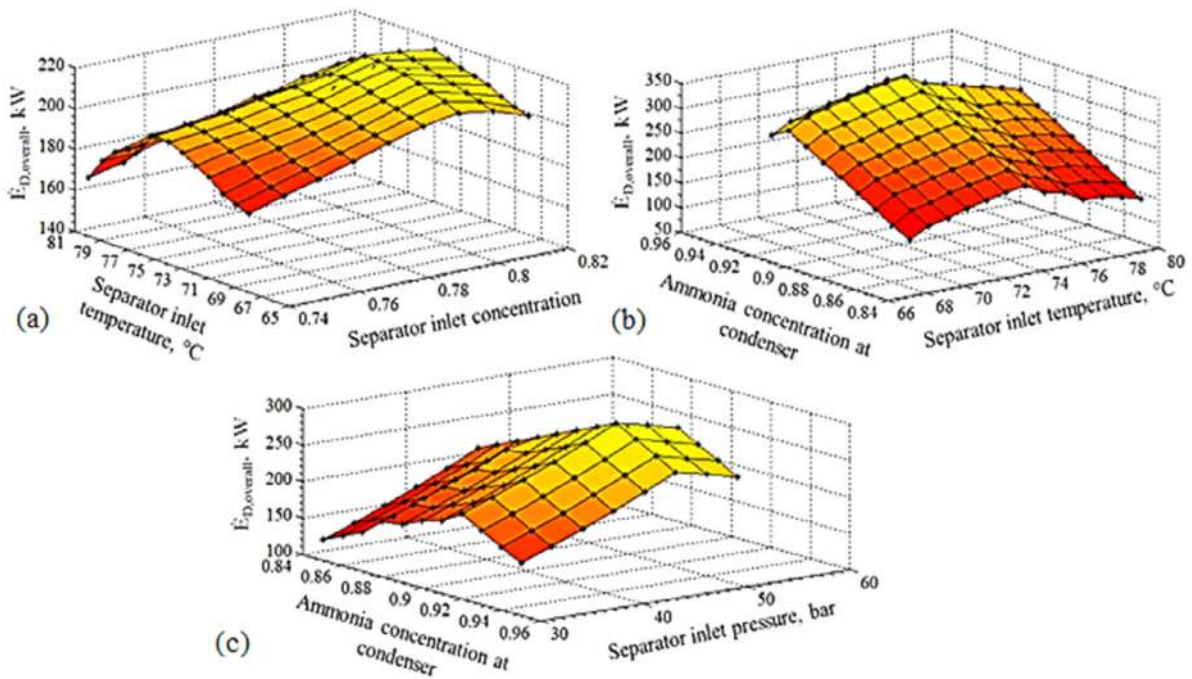


Fig. 8. Effects of (a) separator inlet concentration and separator inlet temperature, (b) separator inlet temperature and ammonia concentration at condenser and (c) ammonia concentration at condenser and turbine inlet pressure on overall cost of exergy destruction of AKCS.

in first law performance. If, the losses have been minimized, the overall energy and exergy performance of the systems still improve.

Table 7 presents energy and exergy property values at each state point of the AKCS. The chemical exergy and physical exergy

relate to the total exergy of the system. The exergy value is essential for evaluating basic exergy and advanced exergy analysis. The product and fuel exergy are estimated at the exergy values of each state point.

Table 8 reports the maximum and minimum values of the objective functions at suitable design variables for the AKCS. The

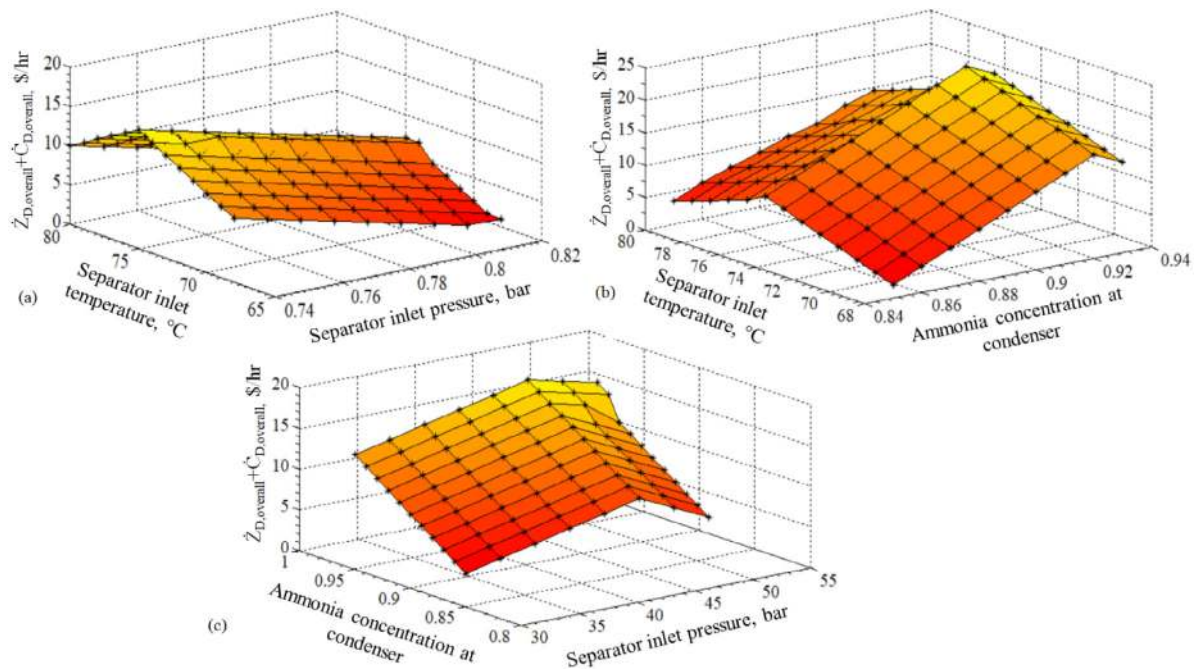


Fig. 9. Effects of (a) separator inlet concentration and separator inlet temperature, (b) separator inlet temperature and ammonia concentration at condenser and (c) ammonia concentration at condenser and turbine inlet pressure on exergoeconomic parameter $(\dot{C}_D + \dot{Z}_D)_{overall}$ of AKCS.

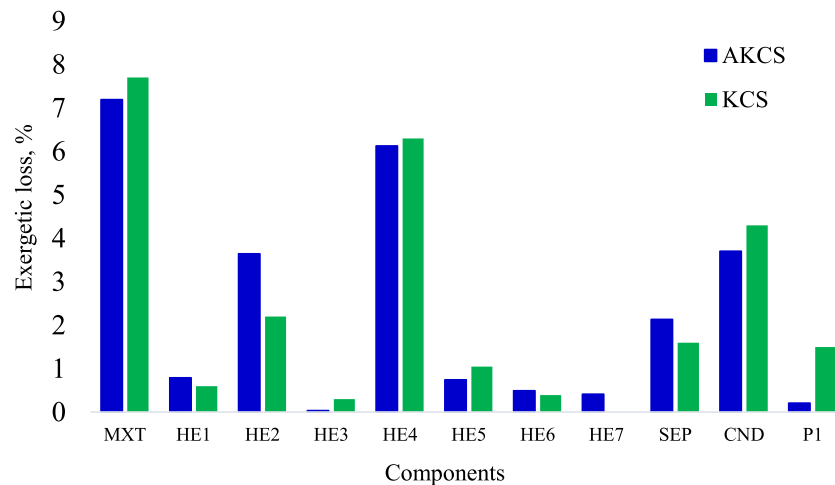


Fig. 10. Comparison of exergetic loss, % of AKCS and KCS.

minimum value of investment cost rate of components, exergy destruction cost rate results at low design variable conditions whereas the maximum value of first and second law efficiencies reports at high design parameter conditions. With the reported parameters the minimized cost values and maximized first law, second law efficiency values have been summarized. The maximum efficiency values and minimum cost values of the AKCS is shown in Fig. 11.

As can be seen from Fig. 12, the components with large relative cost differences are HE₅, turbine, HE₆ and condenser. The low exergoeconomic factor, *f* value for HE₅ represents that the exergy destruction cost is higher in contribution to the total cost resulting high relative cost difference. With low exergoeconomic factor and high relative cost difference the performance can still be improvised by the capital endowment, into an effective system. Hence, with more improved design, the performance of the individual component is optimized. The relative cost difference

for the mixing chambers results with negative signs. The fuel cost of these components is higher than the product cost.

The exergoeconomic factor, *f* for the AKCS components, has been presented in Fig. 13. The least value of exergoeconomic factor results in HE₅ (11.77%) and P₁ (13.33%). The exergoeconomic factor is the ratio of investment cost rate of components and cost of exergy destruction. The large value of ‘*f*’ for the component turbine reveals that the capital cost invested for the turbine has influenced the cost rate connected with exergy destruction in the turbine. The lowest value of exergoeconomic factor reveals that on decreasing the loss in exergy, the savings could be reached. The entire system’s cost effectiveness has been improved by decreasing the exergy destruction of the turbine, HE and the other component’s investment cost

The effects of separator inlet pressure on the summation of investment cost rate of components \dot{Z} , the exergy destruction cost rate \dot{C}_D has been summarized in Table 9. The minimum

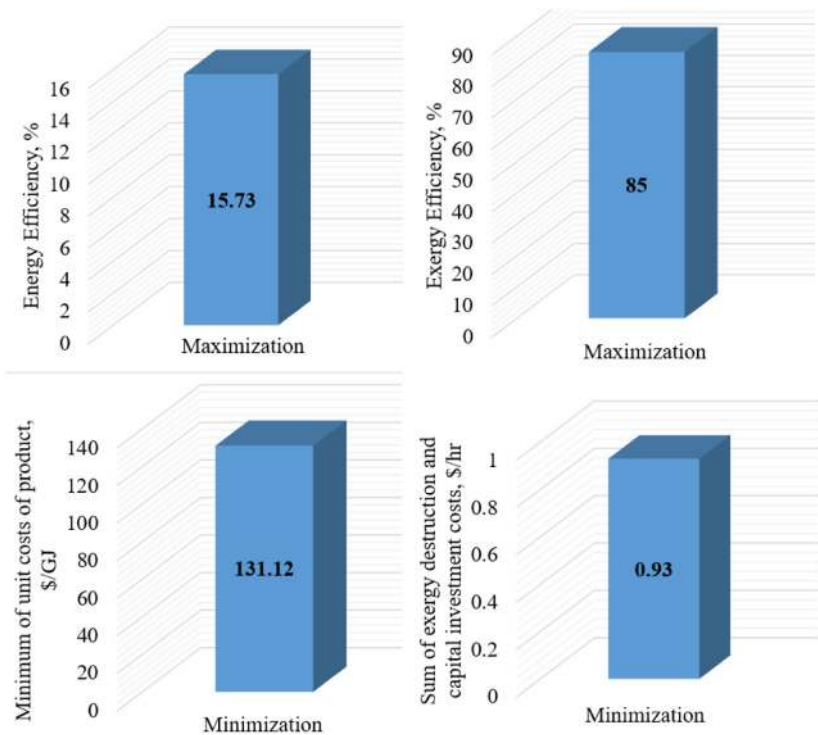


Fig. 11. The ideal efficiency and cost values of AKCS.

Table 7
Thermodynamic property value at each state points of AKCS.

S.No.	P, bar	X	T, °C	m, kg/s	h, kJ/kg	s, kJ/kg K	Chemical exergy, kJ/kg	Physicalexergy, kJ/kg	exergy, kJ/kg
1	43.00	0.80	195.00	1.15	1840.70	5.08	15911.30	333.11	16244.41
2	11.97	0.80	122.00	1.15	1675.00	5.26	15911.30	103.96	16015.26
3	11.97	0.80	75.00	1.15	988.20	3.45	15911.30	-34.77	15876.53
4	11.97	0.98	75.00	0.74	1441.10	4.74	19480.00	27.08	19507.08
5	11.97	0.47	75.00	0.40	99.70	0.92	8971.90	-166.88	8805.02
6	11.97	0.47	75.00	0.25	99.70	0.92	8971.90	-166.88	8805.02
7	11.31	0.47	75.00	0.15	99.70	0.92	8971.90	-166.88	8805.02
8	11.97	0.85	75.00	1.00	1099.10	3.83	16903.00	-35.79	16867.21
9	11.97	0.85	66.50	1.00	1021.60	3.55	16903.00	-41.35	16861.65
10	11.97	0.85	37.00	1.00	66.70	0.54	16903.00	-87.93	16815.07
11	45.00	0.85	38.40	1.00	74.50	0.55	16903.00	-82.46	16820.54
12	45.00	0.85	54.31	1.00	152.00	0.79	16903.00	-64.98	16838.02
13	45.00	0.85	73.77	1.00	250.03	1.08	16903.00	-63.92	16839.08
14	45.00	0.85	73.77	0.94	250.03	1.08	16903.00	-63.92	16839.08
15	45.00	0.85	73.77	0.06	250.03	1.08	16903.00	-63.92	16839.08
16	45.00	0.85	117.00	0.06	1093.00	3.35	16903.00	95.06	16998.06
17	45.00	0.85	117.00	0.93	1093.00	3.35	16903.00	95.06	16998.06
18	45.00	0.85	117.00	1.00	1093.00	3.35	16903.00	95.06	16998.06
19	45.00	0.8	117.00	1.15	947.95	3.00	15911.00	49.81	15960.81
20	45.00	0.8	129.16	1.15	1132.50	3.46	15911.00	103.2	16014.20
21	45.00	0.8	177.81	1.15	1787.00	4.96	15911.00	315.19	16226.19
22	45.00	0.47	76.00	0.15	105.82	0.92	8971.90	-161.28	8810.62
30	5.00	0.00	200.00	3.20	731.32	1.92	50.00	163.29	213.29
31	5.00	0.00	195.38	3.20	712.05	1.88	50.00	155.94	205.94
32	5.00	0.00	139.16	3.20	477.08	1.35	50.00	78.99	128.99
33	5.00	0.00	123.30	3.20	410.81	1.19	50.00	60.43	110.43
34	5.00	0.00	119.41	3.20	388.26	1.13	50.00	55.77	105.77
41	5.00	0.00	88.77	1.07	266.49	0.81	50.00	29.40	79.40
42	5.00	0.00	57.31	1.07	135.05	0.43	50.00	11.26	61.26

value of $\dot{Z} + \dot{C}_D$ results from a separator inlet pressure of 30 bar. The summation of exergoeconomic property ($\dot{Z} + \dot{C}_D$) of MXT, HE₂, HE₄, HE₅, CND and P₁ are large compared to the other components as in Fig. 14. The exergoeconomic actor of HE₅ and P₁ are too low and need no focus on performance improvement.

5. Conclusions

The present work apply energy and exergy analysis of the advanced Kalina cycle system for performance improvement. Every component of the AKCS is formulated with cost balance equations along with auxiliary equations. The exergoeconomic variables

Table 8
The ideal performance parameters of AKCS objective functions.

Parameters	Objective Functions			
	Minimum of c_p	Maximum of the energy efficiency	Maximum of the exergy efficiency	Minimum of $(\dot{C}_D + \dot{Z}_D)_{overall}$
Turbine pressure, bar	30	45	45	30
Separator inlet temperature, °C	68	72	72	68
Ammonia concentration at condenser	0.89	0.94	0.94	0.85
Separator inlet concentration	0.79	0.83	0.83	0.82
c_p (S/GJ)	131.12	138.84	139.84	134.12
Energy efficiency, %	13.12	15.73	15.73	13.12
Exergy efficiency, %	84.30	85	85	84.12
$\dot{E}_{D,overall}$, KW	203.66	303.36	303.36	128.16
$(\dot{C}_D + \dot{Z}_D)_{overall}$, \$/hr	3.03	14.03	14.03	0.93
$\dot{Z}_D,overall$, \$/hr	1.82	8.418	8.418	0.558

Table 9
Effect of turbine inlet pressure on investment cost rate of components \dot{Z} , exergy destruction cost rate \dot{C}_D , and the sum of investment cost rate and exergy destruction rate $(\dot{Z} + \dot{C}_D)$ of the AKCS.

Turbine inlet pressure, bar	30	33	36	39	42	45	48	51
\dot{Z} , \$/hr	8.72	9.62	10.52	11.29	12.11	12.92	12.17	11.61
\dot{C}_D , \$/hr	5.31	5.49	5.68	5.80	6.01	6.14	5.98	5.62
$\dot{Z} + \dot{C}_D$, \$/hr	14.03	15.11	16.20	17.09	18.12	19.06	18.15	17.23

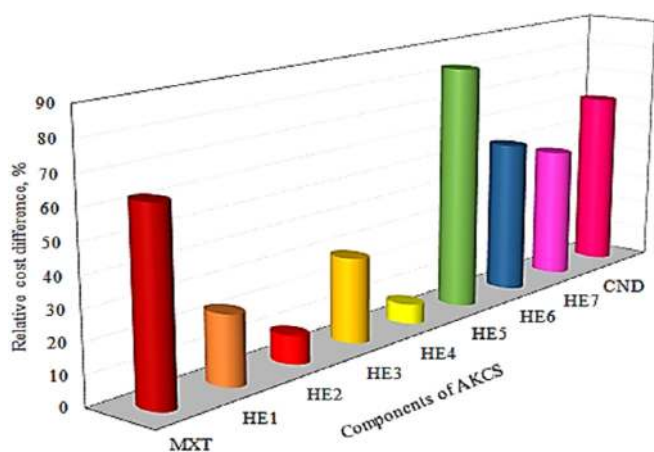


Fig. 12. The relative cost difference, r for components of AKCS.

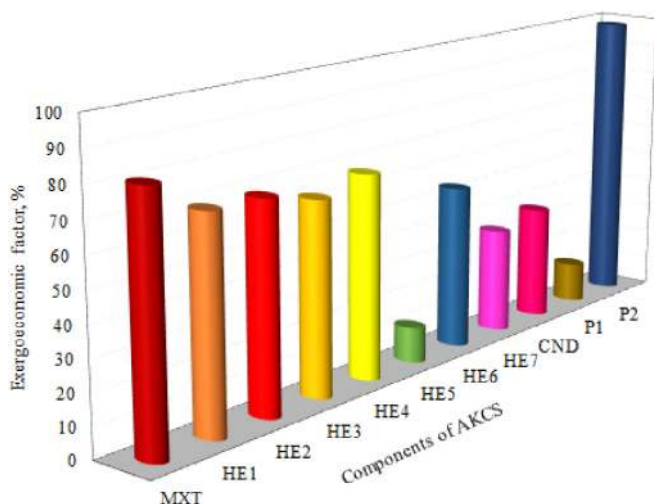


Fig. 13. Exergoeconomic factor, f for components of AKCS.

for the individual components of the AKCS were calculated. The effects of ammonia concentration on condenser, separator inlet concentration, turbine inlet pressure and separator inlet temperature on the investment cost rate of components \dot{Z} , the exergy destruction cost rate \dot{C}_D and the summation of both $(\dot{Z} + \dot{C}_D)$ has been investigated through MATLAB simulation. The conclusion of this work has been summarized as follows

- The energy and exergy efficiency values of the AKCS optimizes at 0.93 ammonia concentration at the condenser and 72 °C separator temperature with 15.7% and 85.5% respectively.
- The total product cost maximizes with a value of 140.12 \$/GJ at 75 °C separator temperature and 0.83 separator inlet concentration.
- The exergy destruction cost rate maximizes with a value of 350.33 kW at 0.92 ammonia concentration on the condenser and 75 °C separator temperature.

The essential accomplishments of this work are listed as concluding remarks.

- The minimum value of the summation of investment cost rate of components \dot{Z} , the exergy destruction cost rate \dot{C}_D results from a separator inlet pressure of 30 bar.
- The components HE₄ and P₁ has got exergoeconomic property $(\dot{Z} + \dot{C}_D)$ of higher values but with the lowest exergoeconomic factor values. Hence these two components have been recommended for performance improvement by capital investment of the improved design.
- The exergoeconomic factor values for components P₂ and turbine are higher, hence requires no recommendations.
- The component HE₅ have got low exergoeconomic factor, f value which ensures that the exergy destruction cost is larger in contribution to the total cost favoring higher relative cost difference. Thus lowering the exergy destruction results in improved individual component performance. This will lead to savings in the overall cost of the system.
- Increasing separator concentration favors no change in the turbine inlet pressure. These results from a reduction of the overall cost of exergy values of the individual components hence favoring a decrement in total cost rate.

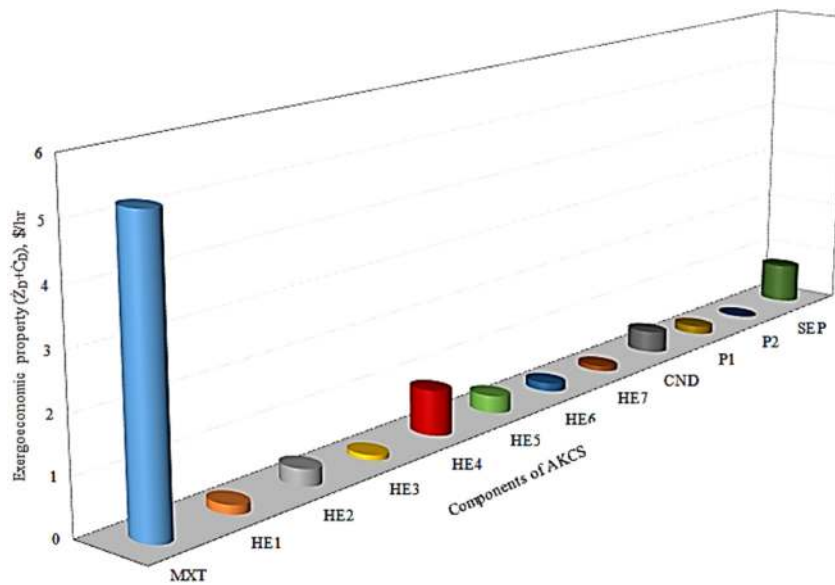


Fig. 14. Exergoeconomic property, $(\dot{Z}_D + \dot{C}_D)$ for components of AKCS.

- The exergoeconomic property $(\dot{C}_D + \dot{Z}_D)$ is minimized at 0.93 \$/hr, 2.04 \$/hr and 4.06 \$/hr at 0.82 separator inlet concentration, 0.85 ammonia concentration at the condenser, 30 bar turbine inlet pressure, and 68 °C separator inlet temperature.

Hence, the ideal performance results are different from energy and thermo-economic analysis of the AKCS. The AKCS has got higher energy and exergy performance values against medium temperature simple Kalina cycle system. The thermo-economic analysis provides recommendations of the components to be improved on cost bases for efficient design.

Nomenclature

Symbols

A_i	Area of individual components, m ²
\dot{m}	mass flow rate, kg/s
h	specific enthalpy, kg/kJ
X	mass fraction of ammonia, kg/kg mixture
T	temperature, K
W	work output, kW
G	generator
M	mechanical
P	pressure, bar
Q	heat supplied, kW
s	specific entropy, kJ/kg K
I	Irreversibility, kJ.kg K
ex	specific exergy, kJ.kg
E	Exergy, kJ
\dot{E}_x	Exergy rate, kW
0	Environment condition
HE	Heat exchanger
MXT	Mixture turbine
SEP	Separator
CND	Condenser
CDP	Condensate pump
CBE	Cost balance equation
AE	Auxiliary equation

F	Vapor fraction
M	Mixing chamber
S	Splitter
Y	exergy destruction ratio, %
\dot{C}	Cost rate (\$/hr)
c	Unit exergy cost (\$/GJ)
CRF	Capital recovery factor
N	annual unit operation hours
\dot{Z}	Investment cost rate of components (\$/hr)
z	Investment cost of components (\$)
r	Relative cost difference (%)
LMTD	Logarithmic mean temperature difference (K)
U	Overall heat transfer coefficient (kW/m ² °C)
VF	Vapor fraction
k	Interest rate
f_i	Exergoeconomic factor

Subscripts

KC	Kalina cycle
ph,i	physical, individual
ch,i	chemical, individual
P	pump
S	supply
KC	Kalina cycle
v	vapor
l	liquid
cwin	cooling water inlet
cwout	cooling water outlet
D	Destruction
F	Fuel
P	Product
tot	total
CI	Capital investment
OM	Operating maintenance
c	Specific exergy cost (\$/GJ)
w	specific work kJ/kg
q	specific heat kJ/kg
R	Reference cost
0	Reference state
i	Individual
is	Isentropic

Greek symbols

η	Efficiency
ε_i	Exergetic efficiency of individual components, %
φ_r	maintenance factor
η_{KC}	Efficiency, Kalina cycle
$\eta_{is, Pump}$	Isentropic Pump Efficiency

CRediT authorship contribution statement

G. Uma Maheswari: Developed computer codes. **N. Shankar Ganesh:** Developed the idea. **Tangellapalli Srinivas:** Manuscript organization, Mathematical solutions. **B.V. Reddy:** Assisted in developing economic models.

Declaration of competing interest

The authors declare that they have no known competing financial interests or personal relationships that could have appeared to influence the work reported in this paper.

Acknowledgment

The authors acknowledge the patent work titled “Thermodynamic cycle based power generation system and a method” Application No.201741046830 A. The authors would like to acknowledge the support received from the management to carry out this research project.

References

- Abam, F.I., Briggs, T.A., Diemuodeke, O.E., Ekwe, E.B., Ujoatuonu, K.N., Isaac, J., Ndukwu, M.C., 2020. Thermodynamic and economic analysis of a Kalina system with integrated lithium-bromide-absorption cycle for power and cooling production. *Energy Rep.* 6, 1992–2005.
- Abdolalipouradi, Mehran, Khalilarya, Shahram, Jafarmadar, Samad, 2019. Exergoeconomic analysis of a novel integrated transcritical CO₂ and Kalina 11 cycles from Sabalan geothermal power plant. *Energy Convers. Manage.* 195, 420–435.
- Bagheri, B.S., Shirmohammadi, R., Mahmoudi, S.M.S., Rosen, M.A., 2019. Optimization and comprehensive exergy-based analyses of a parallel flow double-effect water-lithium bromide absorption refrigeration system. *Appl. Therm. Eng.* 152, 643–653.
- Bahrapoury, R., Behbahani, A., 2017. Thermodynamic optimization and thermoeconomic analysis of four double pressure Kalina cycles driven from Kalina cycle system 11. *Energy Convers. Manage.* 152, 110–123.
- Bejan, A., Tsatsonis, G., Moran, M., 1996. *Thermal Design and Optimization*. Jhon Wiley & Sons, NY, USA.
- Braun, J.E., Bansal, P.K., Groll, E.A., 2002. Energy efficiency analysis of air cycle heat pump dryers. *Int. J. Refrig.* 25 (7), 954–965.
- Cao, L., Wang, J., Chen, L., Dai, Y., 2018. Comprehensive analysis and optimization of Kalina-Flash cycles for low-grade heat source. *Appl. Therm. Eng.* 131, 540–552.
- Cao, L., Wang, J., Dai, Y., 2014. Thermodynamic analysis of a biomass-fired Kalina cycle with regenerative heater. *Energy* 77, 760–770.
- Dhahad, H.A., Hussen, H.M., Nguyen, P.T., Ghaebi, H., Ashraf, M.A., 2020. Thermodynamic and thermoeconomic analysis of innovative integration of Kalina and absorption refrigeration cycles for simultaneously cooling and power generation. *Energy Convers. Manage.* 203, 112241.
- Fallah, M., Mahmoudi, S.M.S., Yari, M., Ghiasi, R.A., 2016. Advanced exergy analysis of the Kalina cycle applied for low temperature enhanced geothermal system. *Energy Convers. Manage.* 108, 190–201.
- Feng, H., Tao, G., Tang, C., Ge, Y., Chen, L., Xia, S., 2019. Exergoeconomic performance optimization for a regenerative closed-cycle gas turbine combined heat and power plant. *Energy Rep.* 5, 1525–1531.
- Ganesh, N.S., Srinivas, T., 2013. Power augmentation in a Kalina power system for a medium temperature low grade heat. *ASME J. Sol. Energy* 135 (3), 1–10.
- Gao, H., Chen, F., 2018. Thermo-economic analysis of a bottoming Kalina cycle for internal combustion engine exhaust heat recovery. *Energies* 11 (11), 3044.
- Ghaebi, Hadi, Namin, Amin Shekari, Rostamzadeh, Hadi, 2018a. Exergoeconomic optimization of a novel cascade Kalina/Kalina cycle using geothermal heat source and LNG cold energy recovery. *J. Cleaner Prod.* 189, 279–296.
- Ghaebi, Hadi, Namin, Amin Shekari, Rostamzadeh, Hadi, 2018b. Performance assessment and optimization of a novel multi-generation system from thermodynamic and thermoeconomic viewpoints. *Energy Convers. Manage.* 165, 419–439.
- Ghaebi, Hadi, Parikhani, Towhid, Rostamzadeh, Hadi, Farhang, Behzad, 2017. Thermodynamic and thermoeconomic analysis and optimization of a novel combined cooling and power (CCP) cycle by integrating of ejector refrigeration and Kalina cycles. *Energy* 139, 262–276.
- Han, X., Li, N., Wu, K., Wang, Z., Tang, L., Chen, G., Xu, X., 2013. The influence of working gas characteristics on energy separation of vortex tube. *Appl. Therm. Eng.* 61 (2), 171–177.
- Junior, E.P.B., Arrieta, M.D.P., Arrieta, F.R.P., Silva, C.H.F., 2019. Assessment of a Kalina cycle for waste heat recovery in the cement industry. *Appl. Therm. Eng.* 147, 421–437.
- Kahraman, M., Olcay, A.B., Sorgüven, E., 2019. Thermodynamic and thermoeconomic analysis of a 21 MW binary type air-cooled geothermal power plant and determination of the effect of ambient temperature variation on the plant performance. *Energy Convers. Manage.* 192, 308–320.
- Khankari, G., Munda, J., Karmakar, S., 2016. Power generation from condenser waste heat in coal-fired thermal power plant using Kalina cycle. *Energy Procedia* 90, 613–624.
- Lazzaretto, A., Tsatsaronis, G., 2006. SPECO: a systematic and general methodology for calculating efficiencies and costs in thermal systems. *Energy* 31 (8–9), 1257–1289.
- Liu, Z., Liu, Z., Cao, X., Luo, T., Yang, X., 2020a. Advanced exergoeconomic evaluation on supercritical carbon dioxide recompression Brayton cycle. *J. Cleaner Prod.* 256, 120537.
- Liu, Z., Liu, B., Guo, J., Xin, X., Yang, X., 2019. Conventional and advanced exergy analysis of a novel transcritical compressed carbon dioxide energy storage system. *Energy Convers. Manage.* 198, 111807.
- Liu, Z., Yang, X., Jia, W., Li, H., Yang, X., 2020b. Justification of CO₂ as the working fluid for a compressed gas energy storage system: A thermodynamic and economic study. *J. Energy Storage* 27, 101132.
- Maheswari G. Uma, Shankar Ganesh, N., 2020. Performance investigation in modified and improved augmented power generation Kalina cycle using Python. *Int. J. Energy Res.* 44 (3), 1506–1518.
- Mahmoudi, S.M.S., Pourreza, A., Akbari, A.D., Yari, M., 2016. Exergoeconomic evaluation and optimization of a novel combined augmented Kalina cycle/gas turbine-modular helium reactor. *Appl. Therm. Eng.* 109, 109–120.
- Mehrpooya, Mehdi, Ghorbani, Bahram, Hosseini, Seyed Sina, 2019. Developing and exergetic performance assessment of biogas upgrading process driven by flat plate solar collectors coupled with Kalina power cycle. *Energy Convers. Manage.* 181, 398–413.
- Mehrpooya, M., Mousavi, S.A., 2018. Advanced exergoeconomic assessment of a solar-driven Kalina cycle. *Energy Convers. Manage.* 178, 78–91.
- Modi, A., Kærn, M.R., Andreasen, J.G., Haglind, F., 2016. Thermoeconomic optimization of a Kalina cycle for a central receiver concentrating solar power plant. *Energy Convers. Manage.* 115, 276–287.
- Mohammadi, A., Ahmadi, M.H., Bidi, M., Ghazvini, M., Ming, T., 2018a. Exergy and economic analyses of replacing feedwater heaters in a rankine cycle with parabolic trough collectors. *Energy Rep.* 4, 243–251.
- Mohammadi, Amin, Ashouri, Milad, Ahmadi, Mohammad Hossein, Bidi, Mokhtar, Sadeghzadeh, Milad, Ming, Tingzhen, 2018b. Thermoeconomic analysis and multiobjective optimization of a combined gas turbine, steam, and organic Rankine cycle. *Energy Sci. Eng.* 6 (5), 506–522.
- Ozahi, E., Tozlu, A., 2020. Optimization of an adapted Kalina cycle to an actual municipal solid waste power plant by using NSGA-II method. *Renew. Energy* 149, 1146–1156.
- Parikhani, Towhid, Azariyan, Hossein, Behrad, Reza, Ghaebi, Hadi, Jannatkah, Javad, 2020. Thermodynamic and thermoeconomic analysis of a novel ammonia-water mixture combined cooling, heating, and power (CCHP) cycle. *Renew. Energy* 145, 1158–1175.
- Parikhani, T., Jannatkah, J., Shokri, A., Ghaebi, H., 2019. Thermodynamic analysis and optimization of a novel power generation system based on modified Kalina and GT-MHR cycles. *Energy Convers. Manage.* 196, 418–429.
- Rashidi, Jouan, Yoo, Chang Kyoo, 2017. Exergetic and exergoeconomic studies of two highly efficient power-cooling cogeneration systems based on the Kalina and absorption refrigeration cycles. *Appl. Therm. Eng.* 124, 1023–1037.
- Rashidi, Jouan, Yoo, ChangKyoo, 2018. Exergy, exergo-economic, and exergy-pinch analyses (EXPA) of the Kalina power-cooling cycle with an ejector. *Energy* 155, 504–520.
- Safarian, S., Aramoun, F., 2015. Energy and exergy assessments of modified organic rankine cycles (ORCs). *Energy Rep.* 1, 1–7.
- Shankar Ganesh, N., Srinivas, T., 2017. Development of thermo-physical properties of aqua ammonia for Kalina cycle system. *Int. J. Mater. Prod. Technol.* 55 (1/2/3), 113–141.

- Shirmohammadi, R., Soltanieh, M., Romeo, L.M., 2018. Thermoeconomic analysis and optimization of post-combustion CO₂ recovery unit utilizing absorption refrigeration system for a natural-gas-fired power plant. *Environ. Prog. Sustain. Energy* 37 (3), 1075–1084.
- Shokati, Naser, Ranjbar, Faramarz, Yari, Mortaza, 2018. A comprehensive exergoeconomic analysis of absorption power and cooling cogeneration cycles based on Kalina, part 1: Simulation. *Energy Convers. Manage.* 158, 437–459.
- Wang, J., Wang, J., Dai, Y., Zhao, P., 2017. Assessment of off-design performance of a Kalina cycle driven by low-grade heat source. *Energy* 138, 459–472.
- Wang, J., Yan, Z., Zhou, E., Dai, Y., 2013. Parametric analysis and optimization of a Kalina cycle driven by solar energy. *Appl. Therm. Eng.* 50 (1), 408–415.
- Xu, J., Wang, T., Gao, M., Peng, T., Zhang, S., Tan, J., 2020. Energy and exergy co-optimization of IGCC with lower emissions based on fuzzy supervisory predictive control. *Energy Rep.* 6, 272–285.
- Yu, Z., Su, R., Feng, C., 2020. Thermodynamic analysis and multi-objective optimization of a novel power generation system driven by geothermal energy. *Energy* 117381.
- Zare, V., Palideh, V., 2018. Employing thermoelectric generator for power generation enhancement in a Kalina cycle driven by low-grade geothermal energy. *Appl. Therm. Eng.* 130, 418–428.